Rev. Roum. Sci. Techn.– Électrotechn. et Énerg.
Vol.**68**, *4*, pp. 381–387, Bucarest, 2023

ROBUST SENSORLESS SPEED CONTROL OF AN INDUCTION MOTOR DRIVE USING A SYNERGETIC APPROACH

SAMIRA BENAICHA

Keywords: Induction motor; Field-oriented control; Synergetic control; Sensorless speed estimation; Resistance estimation; Model reference adaptive system.

This paper uses a model reference adaptive system (MRAS) to build an improved sensorless rotor-field oriented control (RFOC) induction motor (IM) drive in all speed ranges. However, in the presence of external disturbances and parameter variations, the linear tuning method of the Proportional Integrator (PI) controller in the MRAS adaptation mechanism degrades motor performance. An advanced MRAS-based synergetic technique is proposed to develop two suitable adaptation mechanisms that generate slip speed and stator resistance estimates. The reference and adjustable models are developed in the synchronous rotation coordinate system (d-q frame). The effectiveness of the proposed control algorithm was evaluated under various operating conditions using a specific sensorless IM benchmark and the MATLAB/Simulink software environment.

1. **INTRODUCTION**

Field-oriented control (FOC) requires accurate speed and flux measurement or estimation for the high performance of IM drives [1, 2]. The measurement process is fraught with difficulties, particularly the high cost and fragility of the sensors. Furthermore, the physical environment does not always permit the use of sensors [2]. Sensorless control must be used to lower the cost and volume of the drive system while increasing its reliability [3–5]. In the literature, many types of research have been presented on the speed sensorless IM drive (see examples in [5–9]). These techniques can be classified into two main categories: i) model-based techniques and ii) signal injection methods (see some examples in [8]). The first category is based on mathematical models of the IM, such as model reference adaptive system (MRAS), state observer, and artificial intelligence (see, for example, [10–14]).

The MRAS technique is one of the different adaptive control techniques used for state and parameter estimation. It is the most preferable scheme due to its simple structure and satisfactory performance over a wide range of operations. The fundamental algorithm of the MRAS technique has been introduced by Landau [15]. It consists of a reference model, an adjustable model, and an adaptation mechanism, which adapts the variable estimate based on the error between the two model outputs. More than 275 publications control based on Model Reference Adaptive System electric drives using various motor control techniques were reviewed and presented in [10].

Most of the adaptation mechanisms in MRAS speed observers already discussed in the literature use a fixed-gain linear PI controller. Comprehensive studies are presented in [10,11] to explain the effect of using the PI in adaptation mechanisms. However, due to continuous changes in motor parameters caused by temperature variations, uncertain load disturbances, additional non-linearities in the inverter, and integrator and differentiation terms, the PI-based controller may be unable to produce the required satisfactory performance. To avoid such problems, recent researchers have given more attention to exploring other observer adaptation mechanisms to reduce the speed tuning signal and improve speed estimation performance [10,12–14,16–22].

Studies [17,18] have used a sliding mode to replace the MRAS speed estimator's traditional PI adaptation mechanism, which provides good steady-state and transient performance. However, it produces a chattering effect. To overcome these problems, a discrete-terminal sliding-mode-based MRAS is designed [19]. It is confirmed that the proposed method can maintain effective speed estimation; then stability can be ensured at high speed and avoid chattering phenomena. In [12], the authors present a MRAS speed estimator of an induction motor with a fuzzy-PI controller. However, at some operating points, these solutions cause instability. An optimized genetic algorithm is applied to automatically adjust the PI regulator in the model reference adaptive system, which increases performance, guarantees robustness against parametric variations, and ensures good speed tracking and stability performance over the entire operating range of the induction motor [14]. An improved performance of sensorless speed-based MRAS combined with sliding mode and an adaptive neuro-fuzzy controller is proposed in [13]. A high performance of robustness and tracking of an induction motor's trajectory under various operating conditions, particularly at low speed, is provided. A novel MRAS speed estimator that incorporates the Deadbeat regulator into the adaptation mechanism [20] is proposed. The Deadbeat regulator outperforms the competition in terms of performance, response time, and overshoot during the estimation process. In [21], a new MRAS estimator-based observer is offered. The super twisting sliding mode observer is used for speed estimation, a reference model (rotor time constant estimation), and an adjustable model (stator resistance estimation). A parallel estimation system of stator resistance and rotor speed is suggested [22]. The Lyapunov stability theorem is applied to determine the rotor speed and stator resistance adaptation laws. In research [10], we have access to an excellent and detailed review of speed estimation using the MRAS technique in terms of reference and adaptation model types, adaptation mechanisms, stability problems, and the sensitivity of the MRAS estimators in the presence of IM parameter variations. This review permits us to observe all the advantages and disadvantages of this technique.

In recent years, synergetic control has received a great deal of attention in the nonlinear control of electric machines and has been widely studied and successfully applied in various fields. The popularity of this control methodology can be explained in large part by the fact that it provides a framework for designing stabilizing nonlinear controllers or global optimization for a large class of nonlinear dynamic

LSPIE Laboratory, Electrical Engineering Department University of Batna 2, Algeria, Email: samira.benaicha@univ-batna2.dz

DOI: 10.59277/RRST-EE.2023.68.4.10

cascade systems. Several synergetic approaches have been successfully applied in designing controllers for electrical machines [23,24]. This advanced control method appears to be an excellent alternative for developing robust estimators of electrical machines speed and parameters; however, it is still insufficiently used in this area and is not currently used in MRAS estimation. We can only cite studies in [25] in which the author proposed an observer to estimate the components of the rotor flux-linking vector. A new algorithm for rotor flux and speed estimators based on the synergetic technique is proposed in [26]. This algorithm is deduced by using the standard dynamic motor model represented in the PARK model via macro-variables.

The main contribution of this paper is to improve the performance of a sensorless field-oriented control scheme for induction motor drives using synergetic control. The model reference adaptive system (MRAS) scheme is used to estimate the slip speed and the stator resistance simultaneously. However, the error between the reference and the adjustable models, which are developed in the d-q synchronous reference frame, is used to develop two suitable adaptation mechanisms based on synergetic control (SC) to replace the classical fixed gain PI controller. This conjunction is intended to improve the performance of IM sensorless control, especially at low-speed operations.

This paper is structured as follows: Section 2 provides a brief description of synergetic control theory. Section 3 presents the induction motor's dynamic model and rotor flux-oriented control strategy. Sections 4 and 5 are devoted to the development and design of robust sensorless control using the synergetic approach based on an MRAS estimator. Section 6 presents simulation tests using Matlab/Simulink to validate the proposed approach. Section 7 concludes with some closing remarks.

2. BRIEF CONCEPTS OF SYNERGETIC CONTROL

Synergetic control theory was developed by Anatoly Kolesnikov [27]. This approach permits the analytical design of control laws that not only ensure the global stability of the closed-loop system but also its order reduction by successive decompositions. Furthermore, synergetic control theory allows us to solve many difficult control problems effectively that have not been solved by known conventional methods. Generally, the synergetic control design is based on the macro-variable formation defined according to the system state variables in the form of algebraic relations between these variables, which reflect the characteristics of the design requirements. In the simple case, these macro-variables can be defined as a combination of these state variables and determine the properties of the system's motion. The designer can choose the characteristics of these macro-variables according to the requirements or limitations of some of the states [24–26].

A nonlinear system is described by this differential equation:

$$\dot{x} = f_s(x,t) + g(x,t)u\,, \tag{1}$$

$x = (x_1, x_2 \ldots . x_n)$ is a system state vector; f_s is nonlinear smooth function defining the dynamic evolution of the system; t is the time, and u is a control input.

2. 1. STEP 1: CONCEPTION OF A MANIFOLD.

The formation of macro variables in terms of system state variables is the first step in the synergetic control design eq. (1). These macro-variables can be defined as a combination of the state variables that determine the properties of the system's motion and are selected based on parameters such as the control objective.

The macro variable given in eq. (2) is usually used in synergetic control [27]

$$h(\psi_s) = \psi_s. \tag{2}$$

2.2. STEP 2: CONTROLLER DESIGN.

The objective of the control is to force the system to evolve on the domain chosen by the designer:$\psi_s = 0$.The desired dynamic evolution of the macro-variable is given by [26,27]:

$$T_s\dot{\psi}_s + h(\psi_s) = 0, \tag{3}$$

where T_s represents the design parameter, which specifies the convergence speed of the closed loop system to the manifold to be equal to zero.

The function h must satisfy the following condition to ensure the stability of the functional equation:

$$h(0) = 0. \tag{4}$$

Substitute (1) and (2) into (3), the control law is given by:

$$T_s\frac{d\psi_s}{dt}.(f_s(x,t) + g(x)u) + \psi_s(x) = 0\,. \tag{5}$$

By defining an appropriate macro-variable and choosing the parameter T_s, the control output can be derived from (5):

$$u = u_{eq} + u_{sy}. \tag{6}$$

The term u_{eq} is the equivalent term that drives system states to converge toward the manifold and u_{sy} is the synergetic term that forces system states to remain along the manifold.

$$u_{eq} = -\big(\psi_s(x)g(x)\big)^{-1}\psi_s(x)f(x). \tag{7}$$

$$u_{sy} = -\big(\psi_s(x)g(x)\big)^{-1}T_s^{-1}\psi_s(x). \tag{8}$$

3. VECTOR CONTROL OF INDUCTION MOTOR

3.1. MATHEMATICAL MODEL

The dynamic model of an IM in a synchronous *d-q* reference frame can be described as [1,2]:

- Stator model

$$u_{sd} = R_s.i_{sd} + \sigma L_s\frac{di_{sd}}{dt} - \omega_s\sigma L_s i_{sq} + \frac{d\phi_{rd}}{dt} - \omega_s\frac{M}{L_r}\phi_{rq} \tag{9}$$

$$u_{sq} = R_s.i_{sq} + \sigma L_s\frac{di_{sq}}{dt} + \omega_s\sigma L_s i_{sd} + \frac{d\phi_{rq}}{dt} + \omega_s\frac{M}{L_r}\phi_{rd}\,. \tag{10}$$

- Rotor model

$$0 = \frac{M}{T_r}.i_{sd} + \frac{1}{T_r}\phi_{rd} + \frac{d\phi_{rd}}{dt} - (\omega_s - \omega).\phi_{rq} \tag{11}$$

$$0 = \frac{M}{T_r}.i_{sq} + \frac{1}{T_r}\phi_{rq} + \frac{d\phi_{rq}}{dt} - (\omega_s - \omega).\phi_{rd}\,. \tag{12}$$

- Electromagnetic torque

$$\begin{aligned} T_e &= n_p\frac{M}{L_r}\big(\phi_{rd}i_{sq} - \phi_{rq}i_{sd}\big) \\ T_e - T_l &= n_p\left(J\frac{d\omega}{dt} + f_v\omega\right) \end{aligned}, \tag{13}$$

where ϕ is the flux linkage, u is the voltage, i is the current, L is the inductance; $\sigma = (1 - M^2/L_sL_r)$ is the motor leakage coefficient, M is the mutual inductance; R is the resistance, T_r is the rotor time constant, ω is the rotor angular speed, ω_s is the synchronous angular speed, J is the moment of inertia, f_v the friction coefficient, T_l represents the load torque, and n_p

number of pole pairs. The subscripts *r* and *s* denote the rotor and stator values, respectively referred to the synchronous rotating reference frame denoted the d-q-axis.

3.1. ROTOR FIELD-ORIENTED CONTROL

For rotor field-oriented (RFO) control, the rotor flux vector is aligned with d-axis and sets the rotor flux to be constant and equal to the rated flux, which means [1]

$$\phi_{rd} = \phi_r \, , \phi_{rq} = 0. \tag{14}$$

The (IM) model (eqs. (9–13), after field-oriented transformation when we use the constraints (14), can be

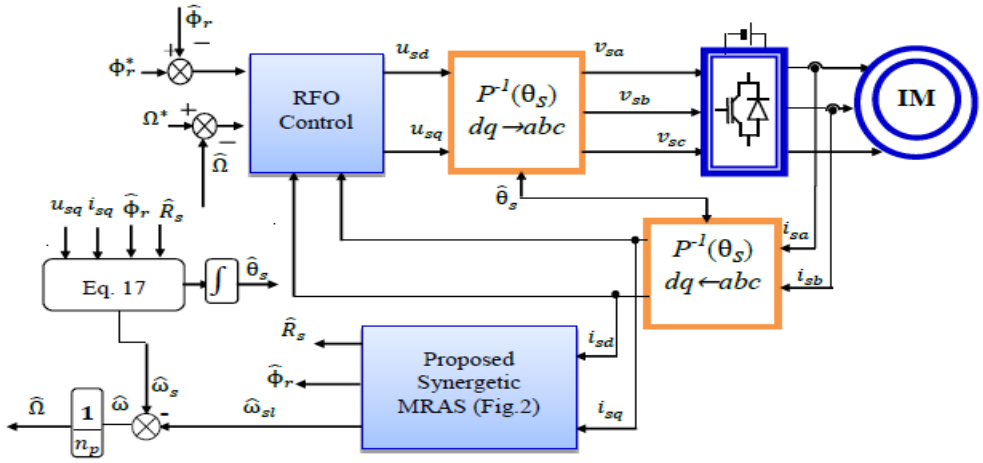

Fig. 1 – Schematic diagram of the sensorless rotor field-oriented control of induction motor.

expressed in a stator rotating frame by the flowing equations:

$$\begin{cases} u_{sd} = R_s i_{sd} + \sigma L_s \frac{i_{sd}}{dt} - \omega_s \sigma L_s i_{sq} + \frac{M}{L_r} \frac{d\phi_{rd}}{dt} \\ u_{sq} = R_s i_{sq} + \sigma L_s \frac{i_{sq}}{dt} + \omega_s \sigma L_s i_{sd} + \omega_s \frac{M}{L_r} \phi_{rd} \\ 0 = \frac{M}{T_r} i_{sd} + \frac{1}{T_r} \phi_{rd} + \frac{d\phi_{rd}}{dt} \\ 0 = \frac{M}{T_r} i_{sq} + - (\omega_s - \omega) \phi_{rd} \\ T_e = n_p \frac{M}{L_r} (\phi_{rd} i_{sq}) \\ T_e - T_l = n_p \left(J \frac{d\omega}{dt} + f_v \omega \right) \end{cases} . \tag{15}$$

The mathematical formulation of the model (15) will be used to elaborate the rotor flux-oriented control [2].

The rotor flux position θ_s required from the coordinate's transformation is generated by the stator pulsation ω_s:

$$\theta_s = \int_0^t \omega_s \, dt. \tag{16}$$

where ω_s can be obtained using the implicit frame orientation technique proposed in [1]:

$$\omega_s = M \frac{u_{sq} - R_s i_{sq} - \sigma L_s (di_{sq}/dt)}{L_s \phi_r}. \tag{17}$$

4. STRUCTURE OF SENSORLESS ROTOR FIELD-ORIENTED CONTROL

The block diagram for a sensorless rotor field-oriented control of an induction motor with stator resistance estimation is shown in Fig 1. To achieve high performance of the RFOC, a conjunction of the MRAS technique with synergetic control is used.

The proposed rotor speed estimation includes the estimation of slip speed $\hat{\omega}_{sl}$ generated by the MRAS technique and synchronous speed ω_s, eq. (17):

$$\hat{\omega} = \omega_s - \hat{\omega}_{sl}. \tag{18}$$

Equation (17) shows that the stator resistance variation of an induction motor causes the control strategy to be inaccurate and doesn't guarantee the decoupling between torque and flux components, especially at very low speed. It is necessary to provide an estimator of $\hat{R}_s$.

5. SIMULTANEOUS SLIP SPEED AND STATOR RESISTANCE ESTIMATION BASED MRAS

The model reference approach (MRAS) uses two distinct models to estimate the same state variable based on different sets of input variables [10,11]. The reference model is independent of the estimated variables, whereas the adjustable model depends directly or indirectly on the estimated variables. The schematic diagram of the slip speed $\hat{\omega}_{sl}$ and the stator resistance $\hat{R}_s$ estimation is presented in Fig. 2.

5.1. REFERENCE AND ADJUSTABLE MODELS

5.1.1. Reference model

The field-oriented constraint ($\phi_{rq} = 0$) is used in the MRAS structure by considering it as a reference model [28]

$$\phi_{rq\_ref} = 0. \tag{19}$$

5.1.2. Adjustable models

In *d-q* synchronously rotating frame, the current and the voltage models are obtained from (15):

- Adjustable model 1: current model

$$\begin{cases} \dot{\hat{\phi}}_{rd} = \frac{M}{T_r} i_{sd} - \frac{1}{T_r} \hat{\phi}_{rd} + \hat{\omega}_{sl} \hat{\phi}_{rq} \\ \dot{\hat{\phi}}_{rq} = \frac{M}{T_r} i_{sq} - \frac{1}{T_r} \hat{\phi}_{rq} - \hat{\omega}_{sl} \hat{\phi}_{rd} \end{cases} . \tag{20}$$

- Adjustable model 2: voltage model

$$\begin{cases} \dot{\phi}_{rd} = \frac{L_r}{M} \begin{pmatrix} u_{sd} - \hat{R}_s i_{sd} - \sigma L_s i_{sd} + \\ \omega_s \sigma L_s i_{sq} + \omega_s \frac{M}{L_r} \phi_{rq} \end{pmatrix} \\ \dot{\phi}_{rq} = \frac{L_r}{M} \begin{pmatrix} u_{sq} - \hat{R}_s i_{sq} - \sigma L_s i_{sq} - \\ \omega_s \sigma L_s i_{sd} - \omega_s \frac{M}{L_r} \phi_{rd} \end{pmatrix} \end{cases} . \tag{21}$$

By using eq. (19) to (21), we can identify the slip speed $\hat{\omega}_{sl}$ and the stator resistance $\hat{R}_s$. Two independent rotor flux estimators are built. The first is obtained by integrating the eq. (21), the second flux estimator appears by using eq. (20). It is noticed that eq. (21) contains the parameter R_s and (20) comprises ω_{sl}. Therefore, the two models can be considered as the adjustable models. Equation (19) does not contain the parameters ω_{sl} and R_s, consequently, it can be considered as a reference model to estimate $\hat{\omega}_{sl}$ and $\hat{R}_s$.

The errors between the reference and the adjustable models are used to drive two suitable adaptation mechanisms that generate the estimation of $\hat{\omega}_{sl}$ and $\hat{R}_s$ using a synergetic control.

5.2. ADAPTION MECHANISMS

5.2.1. Slip speed adaption mechanism

The error between (15) and (16) can be given as:

$$e_{\omega_{sl}} = \phi_{rq-ref} - \hat{\phi}_{rq}. \tag{22}$$

The error $e_{\omega_{sl}}$ is driven to zero by an adaptation mechanism based synergetic approach which yields the estimated rotor speed. The synthesis of the adaptation mechanism is determined by setting the following macro variable:

$$\psi_{\omega_{sl}} = e_{\omega sl} + K_{I1} \int e_{\omega_{sl}} dt\,. \tag{23}$$

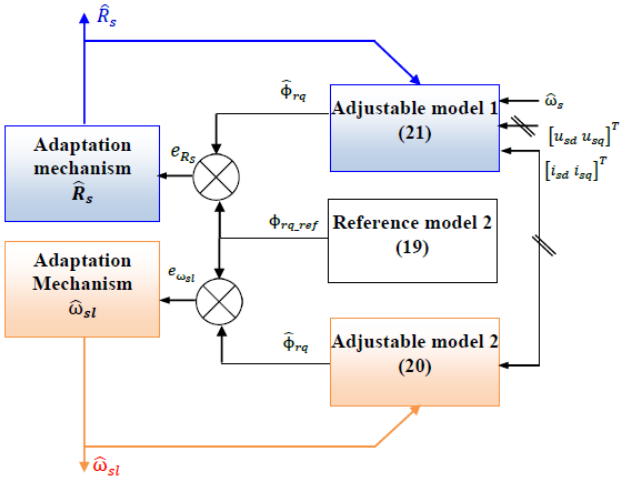

Fig. 2 –Slip speed and stator resistance estimation based on synergetic technique.

K_{I1} is a positive constant that should be tuned properly. When the slip speed error is small, K_{I1} is adjusted to reduce its value; however, a minimum value of zero errors must be set for K_{I1} to obtain a stable estimation of ω_{sl}. The derivatives of $\psi_{\omega_{sl}}$ and $e_{\omega_{sl}}$can be calculated by (24) and (25):

$$\dot{\psi}_{\omega_{sl}} = \dot{e}_{\omega_{sl}} + K_{I1} e_{\omega_{sl}}. \tag{24}$$

$$\dot{e}_{\omega_{sl}} = -\dot{\hat{\phi}}_{rq} = -\frac{M}{T_r} i_{sq} + \frac{1}{T_r}\hat{\phi}_{rq} + \hat{\omega}_{sl}\hat{\phi}_{rd}. \tag{25}$$

Equation (25) can be written as follows:

$$\dot{e}_{\omega_{sl}} = \alpha_\omega + \hat{\omega}_{sl}\beta_\omega. \tag{26}$$

The variables α_ω and β_ω are defined by:

$$\begin{cases} \alpha_\omega = -\frac{M}{T_r} i_{sq} + \frac{1}{T_r}\hat{\phi}_{rq} \\ \beta_\omega = \hat{\phi}_{rd} \end{cases}. \tag{27}$$

The objective of synergetic approach is to force the system to run on the manifold $\psi_{\omega_{sl}} = 0$. The desired dynamic evolution of the macro-variable is given according to the following equation:

$$T_{\psi_1}\dot{\psi}_{\omega_{sl}} + \psi_{\omega_{sl}} = 0, \quad T_{\psi_1} > 0. \tag{28}$$

The constant T_{ψ_1} represents the rate of convergence of the macro-variable to manifold $\psi_{\omega_{sl}} = 0$:

Substituting (26) in (24) and using (28), we get:

$$\begin{aligned} &(\alpha_\omega + \hat{\omega}_{sl}\beta_\omega) + K_{I1} e_{\omega_{sl}} + \\ &+ \frac{1}{T_{\psi_1}}\left(e_{\omega_{sl}} + K_{I1}\int e_{\omega_{sl}} dt\right) = 0 \end{aligned} \tag{29}$$

By solving (29), the estimated slip speed is expressed as:

$$\hat{\omega}_{sl} = \frac{1}{\beta_\omega}\begin{pmatrix} -\alpha_\omega - K_{I1} e_{\omega_{sl}} \\ -\frac{1}{T_{\psi_1}}\psi_{\omega_{sl}}(e_{\omega_{sl}}) \end{pmatrix} = \hat{\omega}_{eq} + \hat{\omega}_{sy}, \tag{30}$$

where, $\hat{\omega}_{\mathrm{eq}} = -\frac{1}{\beta_\omega}\left(\alpha_\omega + K_{I1} e_{\omega_{sl}}\right)$ is the estimated equivalent term and $\hat{\omega}_{\mathrm{sy}} = -\frac{1}{\beta_\omega T_{\psi_1}}\psi_{\omega_{sl}}(e_{\omega_{sl}})$ is the synergetic term.

5.2.2. Stator resistance adaption mechanism

The stator resistance estimated $\hat{R}_s$ is generated from the adaptation mechanism using the error between the models (19) and (21) defined as:

$$e_{R_s} = \phi_{rq-ref} - \phi_{rq}. \tag{31}$$

Hence the dynamic of e_{R_s} is given by:

$$\dot{e}_{R_s} = \alpha_R + \hat{R}_s\beta_R. \tag{32}$$

$$\begin{cases} \alpha_{\mathrm{R}} = -\frac{L_r}{M}\left(\mathrm{u_{sq}} - \sigma L_s i_{\mathrm{sq}} - \omega_{\mathrm{s}}\sigma L_s i_{\mathrm{sd}} - \omega_{\mathrm{s}}\frac{M}{L_r}\phi_{\mathrm{rd}}\right) \\ \beta_{\mathrm{R}} = \frac{L_r}{M}\left(\mathrm{i_{sq}}\right) \end{cases}. \tag{33}$$

$\hat{R}_s$ estimation synergetic synthesis starts with the definition of a macro-variable given by:

$$\psi_{R_s} = e_{R_s} + K_{I2}\int e_{R_s} dt \tag{34}$$

The dynamic of the evolution of the macro-variable ψ_{R_s} is defined by:

$$T_{\psi_2}\dot{\psi}_{R_s} + \psi_{R_s} = 0; \quad T_{\psi_2} > 0. \tag{35}$$

Using the same steps as $\hat{\omega}_{sl}$ calculation, the estimate stator resistance $\hat{R}_s$is given by the flowing expression:

$$\hat{R}_s = \frac{1}{\beta_R}\left(-\alpha_R - K_{I2} e_{R_s} - \frac{1}{T_{\psi 2}}\psi_{R_s}(e_{R_s})\right). \tag{36}$$

Equation (36) can take the following form:

$$\hat{R}_s = \hat{R}_{eq} + \hat{R}_{sy}. \tag{37}$$

The obtained stator resistance estimation comprises two terms given by:

$$\begin{cases} \hat{R}_{eq} = -\frac{1}{\beta_R}\left(\alpha_R + K_{I2} e_{R_s}\right) \\ \hat{R}_{sy} = -\frac{1}{\beta_R T_{\psi 2}}\psi_{R_s}(e_{R_s}) \end{cases}. \tag{38}$$

6. TESTS IN SIMULATION

MATLAB/Simulink software was used to illustrate the performances of sensorless control algorithm shown in Fig. 1. The induction motor parameters are listed in Table 1. The simulation results are presented for the following two tests.

Table 1
Induction Motor Parameters

Nominal rate power	4 kW	R_s	1.8 Ω
Nominal rotor speed	1440 rpm	R_r	1.2 Ω
Nominal current	15/8.6 A	L_s, L_r	0.1564 H
Nominal Voltage	220/380 V	M	0.1500 H
Number of pole pairs	2	J, f_v	0005 kg.m^2, 0.001 Nms/rad

6.1. FIRST TEST: TRACKING PERFORMANCE

In this case, the rotor resistance and stator resistance are assumed to be nominal values regardless of speed change or load change. The sensorless control benchmark Fig.3 proposed by [29] describes the appropriate reference trajectories to check the effectiveness and the performance of the sensorless control algorithm. In this benchmark, different phases are presented:

- Phase 1from 1s to 3 s: Low speed (20 rad/s) with nominal load applied from 1.5 to 2 s
- Phase 2 from 4 s to 6 s: High speed (100 rad/s) with nominal load applied from 5 s.
- Phase 3 from 7 s to 9 s: Very low and negative speed (zero frequency) with nominal load.

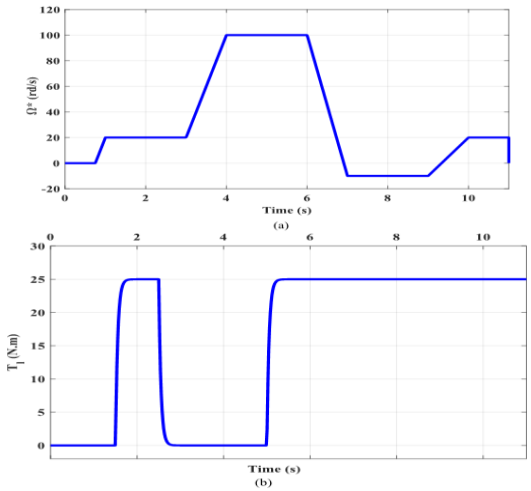

Fig. 3 – Benchmark trajectories; a) reference speed; b) load charge.

Figure 4 illustrates the first test simulation results for sensorless SC of IM according to significant benchmark Fig. 3. It shows very good performance in speed, torque, fluxes, and currents. The system remains stable with a decoupling control between torque and flux, and a rapid reject at the moment of disturbance load torque is applied with small static error; these good performances are achieved at low speed and high speed when the load torque is set at nominal load $T_l = 25$ N · m on t =1.5 s and t = 5 s. The slip speed (Fig. 4a?), has the same form as the stator current i_{sq} effectively proves the law control (eq. (24)).

Figures 4b and c show simultaneously the rotor speed and speed error. It can be noted that the estimated speed given by synergetic MRAS and the actual speed is in good agreement, and the estimation error is small. In Fig. 4c, we observe a good rotor flux orientation (q-axis flux ϕ_{rq} is maintained at zero, d-axis flux ϕ_{rd} corresponds to the reference flux ϕ_r^* =1Wb) with a minor error (see Fig. 4d). In Fig. 4e, the developed electromagnetic torque by IM has a high dynamic with a fast response and tracks exactly the imposed step changes of the load torque.

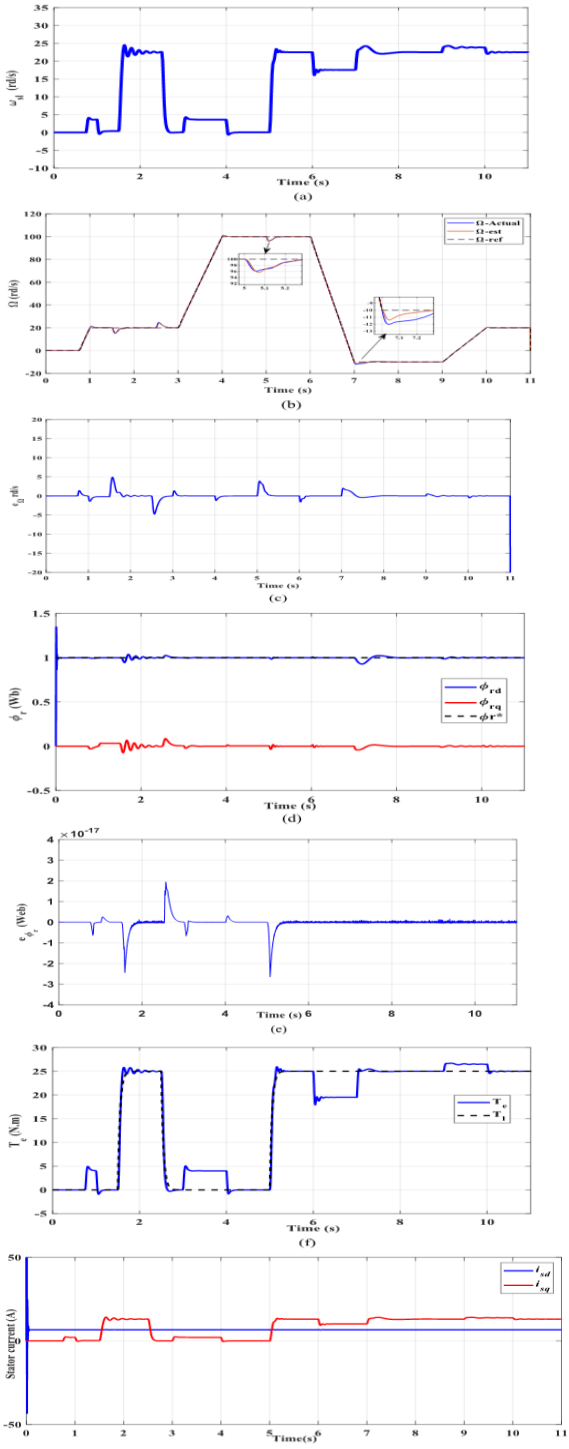

Fig. 4 – Test 1 tracking performance: a) slip speed; b) rotor speed; c) error speed; d) rotor fluxes; e) error flux; f) electromagnetic torque; g) stator current.

The direct and quadratic stator currents (i_{sd}, i_{sq}) in the synchronous frame are exposed in Fig. 4f. It is obvious that the direct stator current (i_{sd}), which takes a constant value, is similar to that the rotor flux and presents an image of the latter However, the quadratic stator current (i_{sq}), is proportional to the electromagnetic torque and follows the load torque.

6.2. SECOND TEST: STATOR RESISTANCE VARIATION

To evaluate the robustness of the proposed sensorless control, it is important to check the influence of the stator

resistance. Figure 5 shows the online tuning for the stator resistance identification by the parallel MRAS. R_s is increased to 1.2 Ω (rated value) at 1.8 Ω, at t = 2 s, R_s is equal to 0.4 (a decrease of 40 % from the nominal value), and finally, R_s is immediately increased to the rated value.

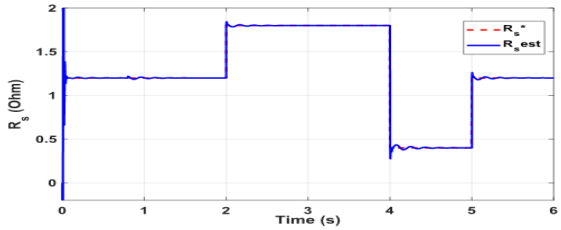

Fig. 5 – Reference and estimation of stator resistance.

During this test, the speed is set to 20 rad/s, and a rated load (T_l =25 N m) is applied. The tracking performance of the rotor resistance estimation for a step change of reference resistance has been shown in Fig. 6.

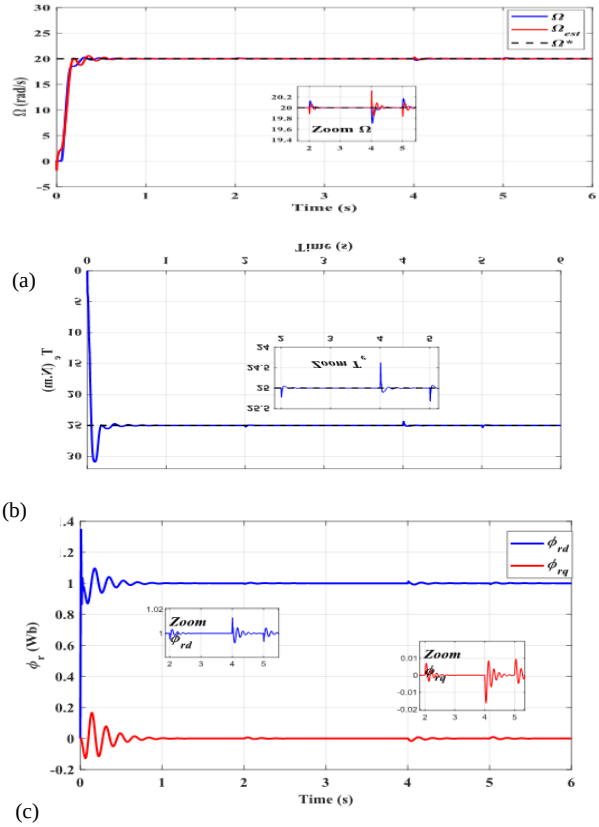

Fig. 6 – Test 2 stator resistance variation: a) rotor speed; b) electromagnetic torque; c) rotor fluxes.

From Figs. 6a, c, we have recorded a good response for electromagnetic torque, rotor speed, and rotor flux when minor errors for the speed and rotor flux are registered. These results confirm that the control scheme, even at low speeds, has good robustness and tracking performance.

7. **CONCLUSION**

A new parallel MRAS based on the synergetic technique has been proposed and tested for speed sensorless rotor field-oriented control of induction motors. The proposed rotor flux MRAS is based on speed estimation and includes two adaptive mechanisms based on synergetic control, one for slip speed and the other for stator resistance estimation. The parallel rotor speed and stator resistance estimator are used to improve the robustness of sensorless speed control when operating at very low speeds with parameter variation. The simulation results confirm the effectiveness of the proposed algorithm; additionally, accurate estimation of stator resistance and speed is achieved under a variety of operating conditions.

Received on 23 February 2023

REFERENCES

1. R. Benoit, F. Bruno, P. Degobert, J.P. Hautier, *Vector control of induction machines: desensitization and optimisation through fuzzy logic*, Springer-Verlag, London, 2012.
2. G. Alain, J. de Leon-Morales, *Sensorless AC Motor Control: Robust Advanced Design Techniques and Applications*, Springer Cham, (1st ed), 2015.
3. D. Xu, B. Wang, G. Zhang, G. Wang, Y. Yu, *A review of sensorless control methods for AC motor drives*, CES Transactions on electrical machines and systems, **2**, *1*, pp. 104–115 (2018).
4. J. Hole, *State of the Art of Controlled AC Drives without Speed sensors*, International journal of electronics, **80**, *2*, pp. 249–263 (1996).
5. R. Saifi, N. Nait-Naid, A. Makouf, A. Chrifi-Alaoui, S. Drid, *Speed sensorless vector control of induction motor using online neural voltage-current phase difference estimation*, Rev. Roum. Sci. Techn. – Électrotechn. et Énerg, **63**, *4*, pp. 403–409 (2018).
6. P. Combes, F. Malrait, P. Martin,P. Rouchon, *An analysis of the benefits of signal injection for low-speed sensorless control of induction motors*, IEEE International Symposium on Power Electronics, Electrical Drives, Automation and Motion (SPEEDAM)., pp. 721–72, Capri, Italy, June 2016.
7. E. R. Montero, M. Vogelsberger, T. Wolbank, *Sensorless identification of machine saliencies in induction motors in the presence of periodic mechanical disturbances*, 23rd European Conference on Power Electronics and Applications (EPE'21 ECCE Europe), Ghent, Belgium, September 2021.
8. H. Mohan, M. K. Pathak, S. K. Dwivedi, *Sensorless Control of Electric Drives – A Technological Review*, IETE Technical Review, **37**, *5*, pp. 504–528, (2020).
9 H. Feroura, F. Krim,, B. Talbi, A.Laib, A. Belaout, *Sensorless field oriented control of current source inverter fed induction motor drive*, Rev. Roum. Sci. Techn. – Électrotechn. et Énerg, **63**, *1*, pp. 100–105 (2018).
10. M. Korzonek, G.Tarchala, T.O. Kowalska, *A review on MRAS-type speed estimators for reliable and efficient induction motor drives,* ISA Transactions, **93**, pp. 1–13 (2019).
11 R. Kumar, S. Das, P. Syam, A.K. Chattopadhyay, *Review on model reference adaptive system for sensorless vector control of induction motor drives*, IET Electric Power Applications, **9**, *7*, pp. 496–511 (2015).
12. U.A. Kumar, D. Maladhi, S. Gunasekaran, S. Nandakumar, *MRAS for induction motor using fuzzy-PI controller in intelligent manufacturing and energy sustainability*, Proceedings of ICIMES, Singapore, Springer Nature Singapore, pp. 197–204, 2023.
13. D. Fereka, M. Zerikat, A. Belaidi, S. Chekroun, *Performance improvement of ANFIS with sliding mode based on MRAS sensorless speed controller for induction motor drive*, Przegląd Elektrotechniczny, **95** (2019).
14. N. El Ouanjli, S. Mahfoud, M.S. Bhaskar, S. El Daoudi, A. Derouich, M. El Mahfoud, *A new intelligent adaptation mechanism of MRAS based on a genetic algorithm applied to speed sensorless direct torque control for induction motor*, International Journal of Dynamics and Control International Journal of Dynamics and Control, **10**, *6*, pp. 2095–2110 (2022).
15 Y.D. Landau, *Adaptive control: the model reference approach*, IEEE Transactions on Systems, Man, and Cybernetics, **1**, pp. 169–170 (1984).
16. P. Ganjewar, Y. Pahariya, *Modified MRAS approach for sensorless speed control of induction motor for reliability improvement*, International Journal of Information Technology, **14**, *3*, pp. 1595–1602 (2022).
17. J. Li, D. Wang, X. Yang, *Speed sensorless control employing adaptive sliding mode adjustable model MRAS for induction motors at low speed range*, Journal of Physics: Conference Series, IOP Publishing, **1633**, *1*, pp. 012145 (2020).

18. S. J. Rind, S. Javed, Y. Rehman, M. Jamil, *Sliding mode control rotor flux MRAS based speed sensorless induction motor traction drive control for electric vehicles*, AIMS Electronics and Electrical Engineering, **7**, *4*, pp. 354–379 (2023).
19. T. Wang., B.Wang, Y. Yu, D. Xu, *Discrete sliding-mode-based MRAS for speed-sensorless induction motor drives in the high-speed range*, IEEE Transactions on Power Electronics, pp. 1–13, 2023.
20. W. Hamdi, M. Y. Hammoudi, A. Betka, *Sensorless Speed control of induction motor using model reference adaptive system and deadbeat regulator*, Engineering Proceedings, **56**, *1*, p.16 (2023).
21. V. Kousalya, B. Singh, *Optimized reference points based vector control of induction motor drive for electric vehicle*, IEEE Transactions on Industry Applications, **59**, *4*, pp. 4164–4174 (2023).
22. H. Heidari, A. Rassolkin, M.H. Holakooie, T. Vaimann, A. Kallaste, A. Belahcen, A. Lukichev, *Parallel estimation system of stator resistance and rotor speed for active disturbance rejection control of six-phase induction motor*, Energies, **13**, *5*, p. 1121 (2020).
23. M. Boumegouas, B. Kabir, K. Kouzi, *New synergetic scheme control of electric vehicle propelled by six-phase permanent magnet synchronous motor*, Advances in Electrical and Electronic Engineering, **20**, *1*, pp. 1–14, (2022).
24. M. Louri, L.Barazane, *Synergetic speed control of squirrel motor* drives, Rev. Roum. Sci. Techn. – Électrotechn. Et Énerg, **61**, *2*, pp. 111–115 (2016).
25. A. Radionov, A.S. Mushenko, *Estimation of components of rotor flux linkage vector for asynchronous electric drive*, International Russian Automation Conference (RusAutoCon), pp. 1–5, 2018.
26. H. Khelloufi, S. Benaicha, *Robust control of an induction motor with speed and flux estimator based on synergetic approach*, 19th International Multi-Conference on Systems, Signals & Devices (SSD), pp. 2048–2053, 2022.
27. A. Kolesnikov, G. Veselov, A. Kolesnikov, *Modern applied control theory: synergetic approach in control theory*, TRTU, pp. 4477–4479, Moscow, Taganrog, 2000.
28. F. Mehazzem, *Contribution to induction motor control for electric traction.* PhD thesis, Department of Embedded Systems, ESIEE School, Paris Est University, Paris, France, 2010.
29. M. Ghanes, A. Glumineau, L. Loron, *New Benchmark for sensorless induction motor drives and validation of a nonlinear controller using a speed observer*, 31st Annual Conference of IEEE Industrial Electronics Society (IECON), Raleigh, North Carolina, USA, November, 2005.